29
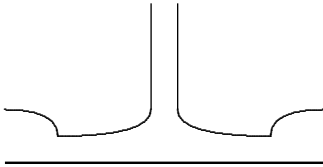
Nonlinear waves

Wading in the water near a beach and fighting to stay upright in the surf, you are evidently under the influence of a nonlinear dynamics, simply because the breaking waves look so different from the smooth swells at the open sea that gave rise to them. Less apparent but equally nonlinear is the dynamics behind the sonic boom caused by a high-speed airplane passing overhead, the short-range shock wave created by an exploding grenade, or the huge atmospheric shock waves created by thermonuclear explosions. The beauty of fluid mechanics lies in the knowledge that all these effects stem from the same nonlinear aspects of the Navier-Stokes equations.
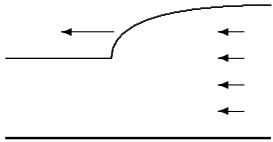
Any linear dynamics has the powerful property that it permits superposition of solutions to the dynamic equations. A complicated solution to a linear dynamics may in the end be completely resolved into a linear combination of elementary solutions. Leaving the domain of linearity this is no more possible, and solutions take on a more individual character. Typically they are difficult to find and demand special techniques in each particular case. They may also be "nasty", unpredictable and chaotic. Nonlinear phenomena have been at focus in physics for most of the 20'th century, and there is still long way to go.

In this chapter the global laws of balance are first used to analyze large-amplitude shallow-water gravity waves, called *hydraulic jumps*, observed every day in the kitchen sink or on the beach. A similar analysis of large-amplitude waves in an isentropic gas reveals the basic physics behind the *shock waves* created by explosions and by supersonic aircraft. Remarkably, it turns out that the nonlinear dynamic equations governing shallow-water surface waves are similar to the nonlinear equations for large-amplitude waves in an isentropic gas, permitting us to see the analogy between hydraulic jumps and shock waves. Deep-water nonlinear surface waves constitute a clean and elegant problem, although they are much harder to deal with. This chapter owes much to [16, 40, 37, 60].
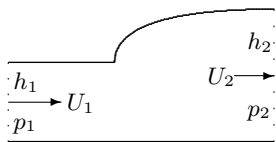
29.1   Hydraulic jumps

A stationary *hydraulic jump* or *step* is easily observed in a kitchen sink. The column of water coming down from the tap splays out from the impact region in a roughly circular flow pattern, and at a certain radius the thin sheet of water abruptly thickens and stays thick beyond. The transition region behind the front appears to have a narrow width and contain quite complicated flow. Strongly turbulent stationary hydraulic jumps may also arise in spillways channelling surplus water from the dam into the river downstream from the dam.

Moving hydraulic jumps are seen on the beach when waves roll in, sometimes in several layers on top of each other. More dramatic *river bores* may be formed by the rising tide near the mouth of a river. When the circumstances are right such waves can roll far up the river with a nearly vertical foaming turbulent front. In the laboratory a bore can be created in a long canal with water initially at rest. When the wall in one end of the canal is set into motion with constant velocity, a bore will form and move down the canal with constant speed and constant water level.

We shall for simplicity analyze a *stationary* jump along a straight line orthogonal to the direction of a uniform horizontal flow. Since one can always choose a frame of reference in which a moving straight-line river bore is stationary, this case is also covered by the following analysis. A gently curved river bore and the stationary circular jump in the kitchen sink are locally nearly straight and thus, at least approximatively, covered.

Sketch of the hydraulic jump in a kitchen sink. The water coming down from the tap splays out in a sheet which suddenly thickens.

A river bore moving in from the right in water initially at rest. The water behind the front moves slower than the front itself.

Stationary jump in planar flow

The flow is assumed to be steady before and after the jump, whereas in the transition region there may be intermittency and turbulence. The Reynolds number is assumed to be so large that viscous friction can be ignored outside the transition region. The liquid streams towards the jump with constant uniform velocity U_1 and constant water level h_1. Downstream from the jump the flow has smaller velocity U_2 and larger water level h_2.

In a control volume containing the transition region, mass conservation guarantees that the rate of mass inflow must equal the rate of outflow. For a stretch L of the straight-line jump we find $\rho_0 U_1 h_1 L = \rho_0 U_2 h_2 L$. Dividing by $\rho_0 L$ this becomes,

$$U_1 h_1 = U_2 h_2 \; , \qquad (29\text{-}1)$$

Sketch of an idealized stationary straight-line hydraulic jump of length L (into the paper). Incompressible fluid enters from the left at velocity U_1 and height h_1 and exits on the right at a lower velocity U_2 and height h_2. The entry and exit pressures, p_1 and p_2, are hydrostatic. At the front the flow pattern is complicated, often turbulent. The control volume encompasses the whole drawing between the dotted lines.

eHydraulicJumpMassBalance

which shows that an increase in height must be accompanied by a drop in velocity.

Momentum balance (16-14) similarly guarantees that the net outflow of momentum from the control volume equals the total external force acting on the control volume. For a nearly inviscid fluid the horizontal force can only be due to the pressure acting on the two vertical sides of the control volume where the liquid enters or leaves. The pressure in the planar flow in these regions is hydrostatic, given by $p_1 = p_0 + \rho_0 g_0 (h_1 - z)$ before the jump and $p_2 = p_0 + \rho_0 g_0 (h_2 - z)$ after,
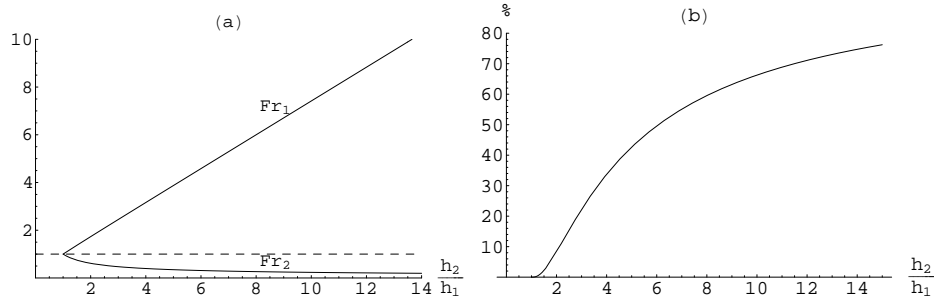
Draft 7.6, December 15, 2003

Figure 29.1: **(a)** *The Froude numbers* $\mathsf{Fr} = U_1/\sqrt{g_0 h_1}$ *before and* $\mathsf{Fr}_2 = U_2/\sqrt{g_0 h_2}$ *after the jump, plotted as function of the height ratio* $h_2/h_1 > 1$. **(b)** *The percentage of the incoming kinetic energy (29-9) dissipated in the stationary jump.*

where p_0 is the constant (atmospheric) pressure on the open surface. Carrying out the force integrals in the usual way, momentum balance becomes (apart from an overall factor $\rho_0 L$),

$$U_2^2 h_2 - U_1^2 h_1 = \frac{1}{2} h_1^2 g_0 - \frac{1}{2} h_2^2 g_0 \ . \tag{29-2}$$

eHydraulicJumpMomentumBalance

On the left one finds the difference between the momentum loss through the outlet and the gain through the inlet of the control volume, and on the right the difference between the total pressure forces acting on the inlet and the outlet.

These equations are solved for U_1 and U_2 with the result,

$$U_1 = \sqrt{\frac{1}{2} g_0 (h_1 + h_2) \frac{h_2}{h_1}} \ , \qquad U_2 = \sqrt{\frac{1}{2} g_0 (h_1 + h_2) \frac{h_1}{h_2}} \ . \tag{29-3}$$

eJumpVelocities

The total mass flow through a stretch of the jump of length L becomes,

$$\dot{M} = \rho_0 U_1 h_1 L = \rho_0 U_2 h_2 L = \rho_0 L \sqrt{\frac{1}{2} g_0 (h_1 + h_2) h_1 h_2} \ , \tag{29-4}$$

eJumpMassFlow

and it is symmetric in h_1 and h_2, as one would expect.

The *Froude number* at the inlet is defined as the ratio of the inlet velocity to the small-amplitude shallow-water wave velocity, $\mathsf{Fr}_1 = U_1/\sqrt{g_0 h_1}$, and similarly at the outlet, $\mathsf{Fr}_2 = U_2/\sqrt{g_0 h_2}$. Inserting the velocities, the Froude numbers become functions only of the ratio h_2/h_1, plotted in fig. 29.1(a),

$$\mathsf{Fr}_1 = \sqrt{\frac{1}{2} \left(1 + \frac{h_2}{h_1}\right) \frac{h_2}{h_1}} \ , \qquad \mathsf{Fr}_2 = \sqrt{\frac{1}{2} \left(1 + \frac{h_1}{h_2}\right) \frac{h_1}{h_2}} \ , \tag{29-5}$$

Since $h_2 > h_1$, we have $\mathsf{Fr}_1 > 1 > \mathsf{Fr}_2$. The inlet velocity is always greater than the shallow-water velocity, whereas the outlet velocity is always smaller. The figure also shows that Fr_1 is very close to being linear in h_2/h_1 whereas Fr_2 is not.

Energy loss in the stationary jump

It would be tempting to make use of Bernoulli's theorem along a streamline going across the stationary hydraulic jump but that is impossible because of the unruly fluid in the transition region which messes up streamlines and generates a dissipative (viscous) loss of mechanical energy.

We may nevertheless use mechanical energy balance (16-91) to calculate the rate of loss of energy from the system by keeping track of what mechanical energy goes into the control volume and what comes out. Mechanical energy balance takes the form (after dividing out the overall factor $\rho_0 L$),

$$\left(\frac{1}{2}U_2^2 + \frac{1}{2}g_0 h_2\right)U_2 h_2 - \left(\frac{1}{2}U_1^2 + \frac{1}{2}g_0 h_1\right)U_1 h_1 = \frac{1}{2}g_0 h_1^2 U_1 - \frac{1}{2}g_0 h_2^2 U_2 - \frac{P}{\rho_0 L} \; .$$
(29-6)

On the left hand side we have the difference between the rates of outflow and inflow of mechanical energy from the control volume, calculated from the mechanical energy density, $\frac{1}{2}\rho_0 \boldsymbol{v}^2 + \rho_0 g_0 z$, integrated over the outlet and inlet. On the right there is first the net rate of work of the pressure forces integrated over the inlet and outlet, and finally P, the rate of loss of energy due to the work of internal friction.

Solving for P we find

$$P = \dot{M}\left(\frac{1}{2}U_1^2 + g_0 h_1\right) - \dot{M}\left(\frac{1}{2}U_2^2 + g_0 h_2\right) = \dot{M}(H_1 - H_2)$$
(29-7)

where $\dot{M}$ is the mass flow (29-4) and H_1 and H_2 are the Bernoulli function (15-16) evaluated at the surface of the water before and after the jump. Substituting the velocities (29-3) we find

$$P = \dot{M}g_0 \; \frac{(h_2 - h_1)^3}{4h_1 h_2} \; .$$
(29-8)

The fraction with dimension of length is what engineers would call the *head loss* (page 271). Since the rate of viscous energy loss must always be positive (page 341), the stationary hydraulic jump must always rise in the downstream direction, $h_2 > h_1$.

A stationary hydraulic jump is perceived as driven by the inflow. Since kinetic energy flows in at a rate $\dot{\mathcal{T}}_1 = \frac{1}{2}\dot{M}U_1^2$, the *fractional dissipative loss* of kinetic energy becomes ,

$$\boxed{\frac{P}{\dot{\mathcal{T}}_1} = \frac{(h_2 - h_1)^3}{(h_1 + h_2)h_2^2} \; .}$$
(29-9)   eJumpDissipation

It is plotted fig. 29.1(b) and converges as expected to unity for $h_2 \rightarrow \infty$. For $h_2/h_1 = 2$, corresponding to $\mathsf{Fr}_1 = 1.73$, only 8.3% of the kinetic energy is lost, whereas for $h_2/h_1 = 10$ corresponding to $\mathsf{Fr}_2 = 7.4$, the fractional loss is 66%. Large hydraulic jumps are efficient dissipators of kinetic energy, and are sometimes used technologically for this purpose, for example in dam spillways.

River bores, reflection bores, and the kitchen sink

The only difference between a river bore and a stationary hydraulic jump lies, as mentioned, in the frame of reference. The river bore is obtained in the frame where the fluid before the jump is at rest. Subtracting U_1 from all velocities (and reversing their directions), the front itself will move with velocity U_1, and the fluid after the jump will move in the same direction with velocity $U_1 - U_2$. This velocity may be larger and smaller than the shallow-water velocity $\sqrt{g_0 h_2}$ and equals it for for $h_2/h_1 \approx 3.21$.

There is also the possibility of choosing a reference frame in which the fluid after the jump is at rest. Subtracting U_2 from the velocities of the stationary jump, this describes to a stationary flow being reflected in a closed canal, forming a *reflection bore* moving with velocity U_2 out of the canal while the flow into the canal has velocity $U_1 - U_2$.

The reflection bore has in fact some bearing on the stationary jump in the kitchen sink, because the spreading circular layer of fluid encounters resistance against the free flow from the sides of the sink or from the slight slope and curvature of its bottom (or even from the increasing viscous friction from the bottom of the thinning layer[1]). This creates a reflection bore which quickly moves towards the center until it gets stopped by the spreading fluid. When the faucet is closed the stationary jump in the kitchen sink immediately turns into a river bore moving towards the center.
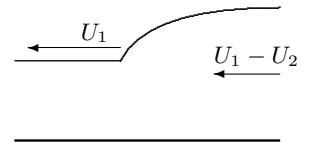
Build-up of a hydraulic jump

A river bore is created by the rising tide at the river mouth, and as long as the tide keeps rising, it will continue to pour more water in. The additional water supplied by the rising tide in a small time interval may be thought of as a small-amplitude surface wave moving upriver on top of the already existing bore. Although this mechanism is most obvious for the river bore, both the reflection bore and the stationary hydraulic jump must also be built up "from behind" by small-amplitude waves.

Any small-amplitude surface wave may be resolved into a superposition of harmonic waves with a spectrum wavelengths. Consider now a harmonic wave with wavelength λ on its way upstream towards a stationary hydraulic jump. In the rest frame of the outflow, the energy in a harmonic wave with wave number $k = 2\pi/\lambda$ moves with the group velocity of a gravity wave (22-31),
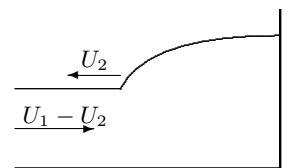
$$c_2 = \frac{1}{2}\sqrt{\frac{g_0}{k}\tanh kh_2}\left(1 + \frac{2kh_2}{\sinh 2kh_2}\right) \ . \qquad (29\text{-}10)$$

In the rest frame of the jump, the wave propagates towards the jump with velocity $c_2 - U_2$ which must be positive if the wave shall ever reach the jump. Since $c_2 \to \sqrt{g_0 h_2}$ for $\lambda \to \infty$ and $U_2 < \sqrt{g_0 h_2}$, this is always possible provided the wavelength exceeds a certain value, $\lambda > \lambda_0$.

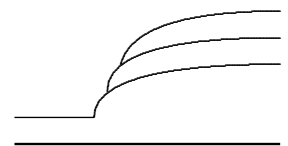[1] T. Bohr, V. Putkaradze, and S. Watanabe, Phys. Rev. Lett. **79**, 1038 (1997).

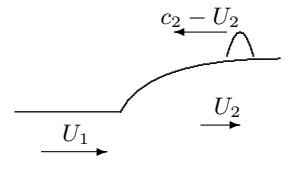*A river bore is obtained by subtracting U_1 from all the velocities of the stationary jump.*

Reflection bore in a closed canal is obtained by subtracting U_2 from all velocities of the stationary jump.

Better to get the 1993 article of Tomas

A river bore is "pumped up" by small-amplitude surface waves of sufficiently long wavelength. Short waves move too slowly to catch up with the jump.

A small amplitude wavelet moving towards the stationary jump with velocity $c_2 - U_2 > 0$.
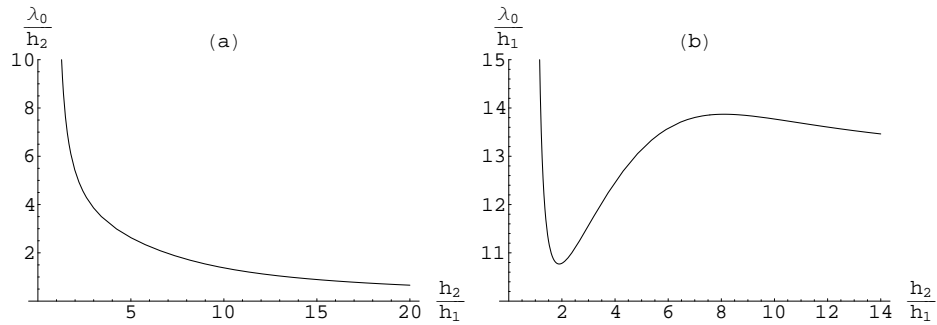
Figure 29.2: **(a)** *The ratio λ_0/h_2 of the minimal wavelength to the height h_2 after the jump as a function of h_2/h_1, obtained by solving (29-11). For $h_2/h_1 \to 1$ the ratio diverges as $\sim (h_2/h_1 - 1)^{-1/2}$, and for $h_2/h_1 \to \infty$ it decreases as h_1/h_2.* **(b)** *The ratio λ_0/h_1 of the minimal wavelength in units of the height h_1 before the jump as a function of h_2/h_1. The minimum $\lambda_0/h_1 \approx 10.77$ occurs for $h_2/h_1 \approx 1.90$, and the maximum $\lambda_0/h_1 \approx 13.87$ for $h_2/h_1 \approx 8.11$. For $h_2/h_1 \to \infty$ the ratio becomes constant, $\lambda_0/h_1 \to 4\pi$.*

The minimal wavelength λ_0 is found by solving the equation $c_2 = U_2$. After division by $\sqrt{g_0 h_2}$ this condition takes the form

$$\frac{1}{2}\sqrt{\frac{\tanh kh_2}{kh_2}}\left(1 + \frac{2kh_2}{\sinh 2kh_2}\right) = \sqrt{\frac{1}{2}\left(1 + \frac{h_1}{h_2}\right)\frac{h_1}{h_2}}\,. \qquad (29\text{-}11) \qquad \text{\scriptsize eJumpCritical}$$

Since the left hand side is only a function of the dimensionless variable $kh_2 = 2\pi h_2/\lambda_0$, this transcendental equation may be solved for λ_0/h_2. The result is shown in fig. 29.2(a) as a function of h_2/h_1. In fig. 29.2(b) the ratio λ_0/h_1 of the wavelength to the water level h_1 before the jump is seen to have a quite dramatic structure.

A smooth hydraulic jump cannot contain details much smaller than the waves that maintain it, so the minimal wavelength λ_0 sets a lower limit to the width of the transition region. For h_2/h_1 only a little above unity fig. 29.2(a) shows that λ_0/h' is large and the jump is barely discernable. For h_2/h_1 between 2 and 3, the width is at least 4 to 6 times h_2. For larger h_2/h_1 the minimal width continues to decrease but the short waves in turbulence may make the front even sharper.

> **Example 29.1.1:** A river bore of height $h_2 = 1$ m moves up a river with depth $h_1 = 0.5$ m. The front velocity calculated from (29-3) becomes $U_1 = 3.8$ m/s and the velocity of the flow behind the front $U_1 - U_2 = 1.9$ m/s. From fig. 29.2(b) we find $\lambda_0/h_1 = 10.8$ for $h_2/h_1 = 2$, so that the minimal wavelength becomes $\lambda_0 = 5.4$ m.

> Check this argument with an expert.

Fig. 29.2(b) reveals something about the character of the hydraulic jump. For $1 \lesssim h_2/h_1 \lesssim 2$, the minimal wavelength decreases rapidly as the jump grows, and each pulse of length λ_0 adds less and less energy, making the jump quite stable. For $2 \lesssim h_2/h_1 \lesssim 6$ the minimal wavelength increases rapidly as the jump grows, and each pulse of length λ_0 adds more energy, making the jump rather unstable. Finally, for $6 \lesssim h_2/h_1 \lesssim \infty$ each pulse adds roughly the same energy and the jump is fairly stable, though with a strongly turbulent front.
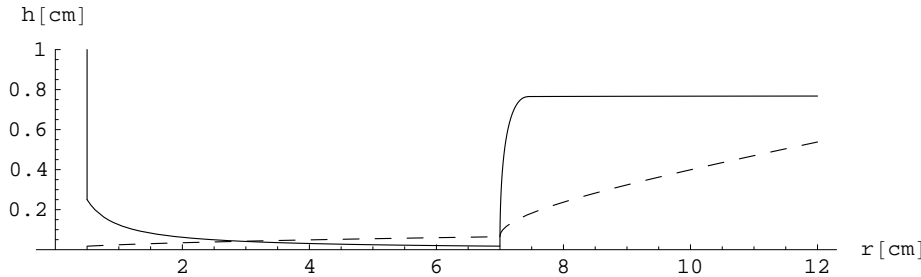
Figure 29.3: *The hydraulic jump discussed in detail in example 29.1.2. The fully drawn line is the water level whereas the dashed line is the estimated thickness of the boundary layer. The fact that it is comparable to the water level in front of the jump indicates that viscosity plays a role in this case, casting some doubts on the validity of the calculation. The jump has been smoothed "by hand" to a width of twice the minimal wavelength. Notice that the height is plotted on a four times larger length scale than the radius.*

Anatomy of the jump in the kitchen sink

The circular stationary hydraulic jump in the kitchen sink is particularly interesting because of the difficulties in predicting where it happens. As discussed above, the position of the jump depends crucially on the forces that resist the free flow towards the drain. Here we shall simply place the jump at a certain radius $r = r_1$ from the center and calculate the shape of the flow before and after, assuming that viscosity can be disregarded. The water is discharged at a volume rate Q from a circular jet of radius r_0, such that its average velocity is $U_0 = Q/\pi r_0^2$. By Bernoulli's theorem the water emerges horizontally with the same speed U_0 as it comes down. Mass conservation, $Q = \pi r_0^2 U_0 = 2\pi r_0 h_0 U_0$, then determines the initial height $h_0 = r_0/2$ of the horizontal sheet of water at $r = r_0$.

Before the jump, $r_0 < r < r_1$, the flow with velocity $U(r)$ and height $h(r)$ is governed by mass conservation together with Bernoulli's theorem for a streamline along the surface,

$$rhU = r_0 h_0 U_0 \ , \tag{29-12}$$

$$\frac{1}{2}U^2 + g_0 h = \frac{1}{2}U_0^2 + g_0 h_0 \ . \tag{29-13}$$

In the general case this becomes a third degree equation for U (or h). When the initial Froude number is large, as in the example below, the potential term $g_0 h$ can be disregarded and the velocity becomes constant, $U \approx U_0$, implying that the height decreases as $h \approx h_0 r_0/r$.

At $r = r_1$ the velocity becomes $U_1 = U(r_1)$ and the height $h_1 = h(r_1)$. The jump transforms these into U_2 and h_2. After the jump we may again use the above equations to determine $U(r)$ and $h(r)$ starting at r_1 with U_2 and h_2. If the Froude number here is small, as in the example below, the height h becomes constant after the jump while the velocity decreases as $1/r$.
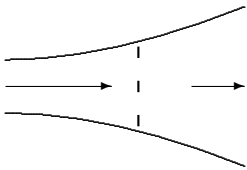
Notice that because of mass conservation across the jump, the Reynolds number $\mathrm{Re} = Uh/\nu = (r_0/r)U_0h_0/\nu$ is continuous and varies inversely with the radius. To test whether the assumption of inviscid flow is justified, one may compare the water level h with a thickness estimate of the boundary layer, for example $\delta = 3\sqrt{\nu r/U}$.

Example 29.1.2 (Kitchen sink jump): In a home-made kitchen sink experiment (see fig. 29.3) the discharge rate was casually observed to be $Q = 100 \ \mathsf{cm}^3/\mathsf{s}$ and the radius of the water column $r_0 = 0.5 \ \mathsf{cm}$. This makes the initial velocity $U_0 = 127 \ \mathsf{cm/s}$ and the initial thickness $h_0 = 0.25 \ \mathsf{cm}$, corresponding to an initial Froude number, $\mathsf{Fr}_0 = 8.1$, and an initial Reynolds number $\mathsf{Re}_0 = 3700$. The radius of the jump was in this case observed to be $r_1 = 7 \ \mathsf{cm}$, but with rapid intermittent variations due to the fluctuations in the water jet from the tap. From the solution of the equations we find $h_1 = 0.018 \ \mathsf{cm}$, $U_1 = 129 \ \mathsf{cm/s}$, corresponding to a Froude number $\mathsf{Fr}_1 = 31$ and a Reynolds number $\mathsf{Re}_1 = 264$. The height ratio (see problem 29.1) becomes $h_2/h_1 = 43.4$, and the height after the jump $h_2 = 0.76 \ \mathsf{cm}$ while the velocity drops to $U_2 = 3 \ \mathsf{cm/s}$, corresponding to a Froude number of $\mathsf{Fr}_2 = 0.11$. The observed height after the jump seems to be a bit smaller than the above prediction. Due to the large height ratio, the minimal wavelength is merely $\lambda_0 = 4\pi h = 0.22 \ \mathsf{cm}$. The jump is indeed quite steep, though perhaps not that steep. In fig. 29.3 the jump has been smoothed to a width of $2\lambda_0$. The boundary layer thickness becomes $\delta_1 = 0.065 \ \mathsf{cm}$ at the jump which is about 4 times the water level. This indicates that viscosity does play some role for this experiment, in particular just before the jump.

29.2 Normal shocks in ideal gases

An explosion in a fluid at rest creates an expanding fireball of hot gases and debris which pushes the fluid in front of it. If the velocity imparted to the fluid by the explosion is smaller than the velocity of sound in the fluid, a sound wave will run ahead of the debris and with a loud bang inform you that the explosion took place. If on the other hand the initial expansion velocity of the fireball is larger than the sound velocity in the fluid, the first sign of the explosion will be the arrival of the supersonic front (here we disregard the flash of light which may arrive much earlier). The sudden jump in the properties of a fluid at the passage of a supersonic front is called a *shock*. Stationary shocks may arise in constricted ducts which choke the flow until it becomes supersonic. The understanding of shocks is of great importance for the design of supersonic aircraft, and of jet and rocket engines.

A stationary shock (dashed) in an expanding nozzle. The inflow is supersonic and the outflow subsonic.

In this section we shall investigate the properties of *normal shocks*, defined as (nearly) singular jumps in the properties of a fluid along a plane orthogonal to the motion of the fluid. Around objects moving at supersonic speeds so-called *oblique* shock fronts will appear, not at right angles with the direction of motion.

The Rankine-Hugoniot relations

We shall later see that normal shocks are in fact not much thicker than the molecular length scale, allowing us to view all normal shocks as singular and locally planar. In the rest system of the shock we choose a narrow control volume just containing an area A of the shock front. Upstream from the shock the gas has velocity U_1, temperature T_1, pressure p_1, and density ρ_1; downstream it has velocity U_2, temperature T_2, pressure p_2, and density ρ_2. Temperature, pressure, and density are of course related by the ideal gas law (4-23) one either side of the shock.

Since the shock is very narrow there will be essentially no space for dissipation of energy, allowing us to balance the energy in addition to mass and momentum. As we have shown in section 16.11 on page 326, energy balance is equivalent to Bernoulli's theorem for an inviscid ideal gas. Using the pressure function (15-32) on page 276 for an ideal gas with adiabatic index γ, we obtain the three basic *Rankine-Hugoniot* relations,
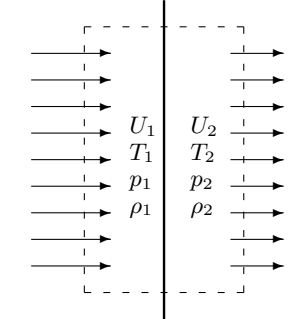
$$\rho_1 U_1 = \rho_2 U_2 \; , \tag{29-14a}$$

$$\rho_1 U_1^2 + p_1 = \rho_2 U_2^2 + p_2 \; , \tag{29-14b}$$

$$\frac{1}{2} U_1^2 + \frac{\gamma}{\gamma - 1} \frac{p_1}{\rho_1} = \frac{1}{2} U_2^2 + \frac{\gamma}{\gamma - 1} \frac{p_2}{\rho_2} \; . \tag{29-14c}$$

A piece of a stationary shock front. Fluid comes in from the left with supersonic velocity U_1, temperature T_1, pressure p_1 and density ρ_1. The fluid emerges on the right with subsonic velocity U_2.

Pierre Henri Hugoniot (1851-1887). *French engineer.*

There is a biography of Hugoniot by Cheret.

These relations are simple rearrangements of mass, momentum, and energy balance across the shock. These equations may be solved explicitly for the downstream parameters in terms of the upstream ones (see problem 29.3). It is, however, more convenient to express the solution in terms of a single dimensionless parameter.

Using (29-14a) to eliminate U_2 in (29-14b), we obtain,

$$U_1^2 = \frac{\rho_2}{\rho_1} \cdot \frac{p_2 - p_1}{\rho_2 - \rho_1} \; , \qquad U_2^2 = \frac{\rho_1}{\rho_2} \cdot \frac{p_2 - p_1}{\rho_2 - \rho_1} \; , \tag{29-15}$$

eRHvelocities

where the second equation is obtained fromt the first by swapping $1 \leftrightarrow 2$. Inserting this into (29-14c) we find the ratio of densities,

$$\frac{\rho_2}{\rho_1} = \frac{\gamma(p_1 + p_2) + p_2 - p_1}{\gamma(p_1 + p_2) + p_1 - p_2} \; . \tag{29-16}$$

This indicates that the dimensionless parameter may conveniently be chosen to be the relative pressure difference across the shock,

$$\tau = \frac{p_2 - p_1}{p_1 + p_2} \; . \tag{29-17}$$

When the absolute pressures are positive (as they must be) this always lies in the interval $-1 < \tau < 1$. In terms of τ, the dimensionless ratios of the physical
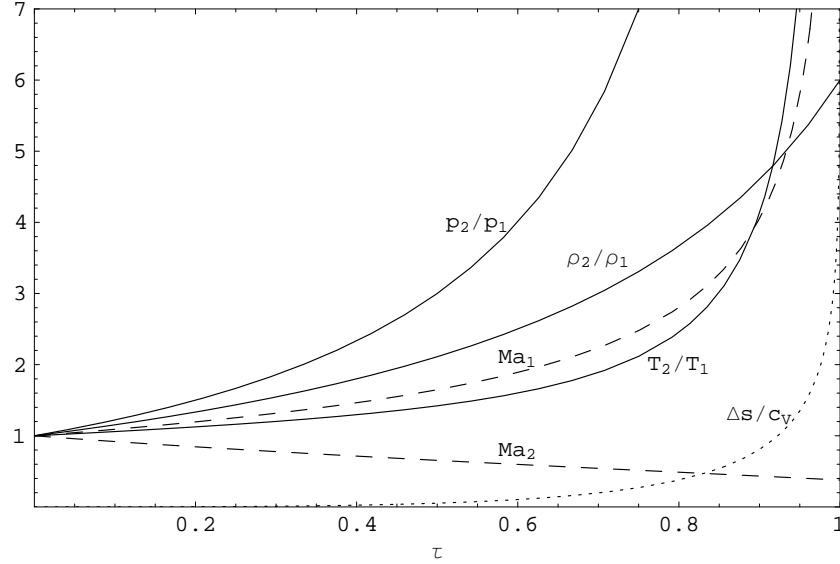
Figure 29.4: *The dimensionless Rankine-Hugoniot parameters as function of the relative pressure jump τ across the shock. The fully drawn curves are the ratios of pressure, density, and temperature. The dashed curves are the Mach numbers Ma_1 and Ma_2, and the dotted curve is the specific entropy jump at the shock, $\Delta s/c_V$ given in (29-22).*

quantities across the shock then become,

$$\frac{p_2}{p_1} = \frac{1+\tau}{1-\tau} \ , \tag{29-18}$$

$$\frac{\rho_2}{\rho_1} = \frac{U_1}{U_2} = \frac{\gamma+\tau}{\gamma-\tau} \ , \tag{29-19}$$

$$\frac{T_2}{T_1} = \frac{1+\tau}{1-\tau} \cdot \frac{\gamma-\tau}{\gamma+\tau} \ . \tag{29-20}$$

Since we are interested in supersonic flow, it is most convenient to express the velocities in terms of the dimensionless Mach numbers, $\mathsf{Ma}_1 = U_1/c_1$ and $\mathsf{Ma}_2 = U_2/c_2$, where $c_1 = \sqrt{\gamma p_1/\rho_1}$ and $c_2 = \sqrt{\gamma p_2/\rho_2}$ are the sound velocities before and after the shock. Using (29-15) we obtain,

$$\mathsf{Ma}_1 = \sqrt{\frac{\gamma+\tau}{\gamma(1-\tau)}} \ , \qquad\qquad \mathsf{Ma}_2 = \sqrt{\frac{\gamma-\tau}{\gamma(1+\tau)}} \ . \tag{29-21}$$

The second equation is obtained from the first by swapping $1 \leftrightarrow 2$ which amounts to changing the sign of τ. All these dimensionless quantities are plotted in fig. 29.4 for $0 \leq \tau \leq 1$.

   Up to this point, everything has been treated symmetrically for the two sides of the shock. The physical asymmetry between the two sides becomes apparent

when we apply the Second Law of Thermodynamics to the change in specific entropy $\Delta s = s_2 - s_1$ across the shock. Using (4-54c) we find,

$$\frac{\Delta s}{c_V} = \log\left[\frac{p_2}{p_1}\left(\frac{\rho_2}{\rho_1}\right)^{-\gamma}\right] = \log\left[\frac{1+\tau}{1-\tau}\left(\frac{\gamma-\tau}{\gamma+\tau}\right)^{\gamma}\right] \ , \qquad (29\text{-}22) \qquad \text{\tiny eRKentropy}$$

where c_V is the specific heat constant of the gas. The right hand side is a monotonically increasing function of τ which vanishes for $\tau = 0$ (see problem 29.4 and fig. 29.4). By the Second Law the specific entropy is not permitted to decrease across the shock, and consequently we must require $\tau > 0$.

What transpires from fig. 29.4 is that the pressure, density, and temperature all increase across the shock, whereas the velocity drops from supersonic ($\mathsf{Ma}_1 > 1$) to subsonic ($\mathsf{Ma}_2 < 1$). The entropy increase is very small for small τ and first reaches c_V at $\tau \approx 0.92$ where $\mathsf{Ma}_1 \approx 4.6$ and $\mathsf{Ma}_2 \approx 0.42$.

Example 29.2.1: